

Behaviour of welded beam-to-column joints subjected to the static load

Davor Skejic[†], Darko Dujmovic[‡] and Boris Androic^{‡†}

Department of Structural Engineering, Faculty of Civil Engineering, University of Zagreb
Kaciceva 26, 10000 Zagreb, Croatia

(Received March 24, 2006, Accepted March 3, 2008)

Abstract. Neglecting the real joint behaviour in frame analysis may result in unrealistic predictions of the response and reliability of steel frames. The reliability of the prediction of main joint properties according to the component method (Eurocode 3-Part 1.8) still remains open to further investigation. The first step toward the solution is to compare the theoretical expressions given in EN 1993-1-8 and the experimental results. With that goal in mind six nominally the same, but really different specimens of welded beam-to-column joints subjected to static load were tested. The specimens present a combination of nominally identical structural elements produced in different European mills. This paper provides these tests, as well as their detailed evaluation and interpretation. All three joint structural properties (rotational stiffness, moment resistance and rotation capacity) have been considered. Four models for determining the plastic resistance out of experimental M_j - ϕ curves have been applied. The results that have been discussed in detail, point to the fact that EN 1993-1-8 underestimates the real structural properties of the tested type of joint, as well as to the conclusion that detailed research of this problem needs to be conducted using the probabilistic reliability methods.

Keywords: semi rigid joint; rotational stiffness; moment resistance; rotation capacity; Eurocode 3-Part 1.8; experimental testing; reliability.

1. Introduction

The component method implemented into EN 1993-1-8: Design of joints, (CEN 2005), allows an analytical and simple evaluation of the main structural steel joint properties. Joint behaviour can generally be represented through a nonlinear moment-rotation (M - Φ) relationship characterized by three main structural properties: moment resistance, rotational stiffness and rotation capacity. Even though in the last few years much research has been conducted and many papers on the rotation capacity of structural joints have been written (da Silva *et al.* 2002, Girao Coelho *et al.* 2004, Beg *et al.* 2004, Girao Coelho *et al.* 2005) there is still no simple analytical procedure to evaluate that structural property. The question of the reliability of moment resistance and rotational stiffness evaluation also arises.

Overestimating the joint stiffness may result in the underestimating of lateral sway, storey drift

[†] Research Assistant, MSc., Corresponding author, E-mail: davors@grad.hr

[‡] Professor, Ph.D., E-mail: dujmovic@grad.hr

^{‡†} Professor, Ph.D., E-mail: androic@grad.hr

and probability of failure, whereas the underestimation of joint resistance can lead to the underestimation of the values and distribution of internal forces and bending moments in beams and columns. Therefore, the accuracy of the main joint structural properties evaluation affects the reliability of joint classification, and in the end, the reliability of steel frames with semi rigid joints. For a global elastic analysis of the steel frame, it is important to reliably classify the joint with regard to rotational stiffness, while the global plastic analysis requires the moment resistance and joint rotation capacity to be known. The component method makes it clear that the variability of real mechanical properties of the material from which the joint elements are made significantly affects the joint moment resistance.

This paper focuses on the experimental evaluation of single-sided welded beam-to-column joint behaviour. The evaluation of experimental results for six nominally identical specimens was also conducted, where the specimens were created by combining beams and columns supplied by various European manufacturers. The procedure for experimental data evaluation, as well as the way in which the experimental M_f - ϕ curves were obtained was also presented in detail. Four models for experimental resistance determination have been applied. Since different models for determining resistance from experimental M_f - ϕ curves can be found in the relevant papers (Girao Coelho *et al.* 2004, Aribert *et al.* 2004), their acceptability for the evaluation of welded single-sided beam-to-column joints was also analyzed.

The obtained results point to the conclusion that a detailed probabilistic analysis of the reliability of joint designed using the component method is necessary. Towards a realistic, as well as simple, semi rigid joint behaviour evaluation the existing component method needs to be upgraded.

2. The description of the experimental programme

2.1 The aim of testing

The aim of the testing conducted was to record the real behaviour of the welded beam-to-column joint by means of the experimental M_f - ϕ curve, and to get the real joint properties with regard to rotational stiffness, moment resistance and rotation capacity. Based on real properties the difference between the semi rigid single-sided welded beam-to-column joint behaviour obtained in experimental testing and the design model proposed by Eurocode 3, Part 1.8 (CEN 2005) was defined.

The tests were conducted on welded single-sided steel beam-to-column joints made out of I-sections subjected to static load. All six specimens are nominally the same, geometrically and mechanically. The beams are made out of IPE 240 and the columns out of HE 200 A sections. All of the specimen members were made out of steel S 235 JR +N according to European Standards EN 10025-2 (CEN 2004) and EN 10204 (CEN 2004). It is important to note that individual sections of beams and columns were supplied by different manufacturers, so that their combinations resulted in six specimens of joints, which are different, though nominally identical.

2.2 Testing plan

2.2.1 The description of the joint specimen

The joint specimen tested was chosen with regard to laboratory conditions, the test frame

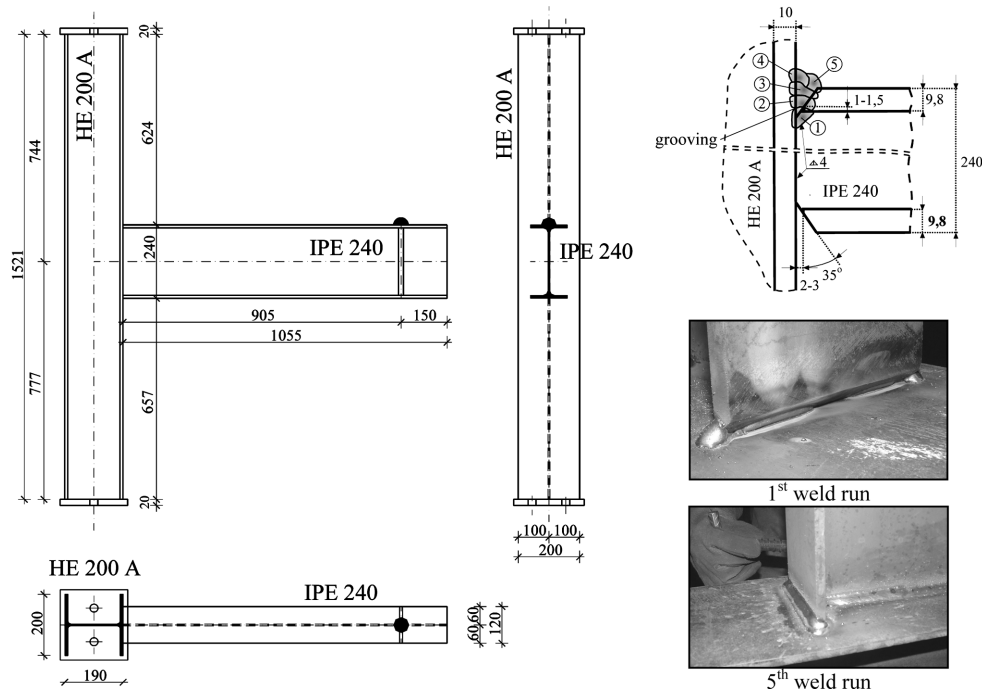


Fig. 1 Welded beam-to-column joint specimen, with manner of weld execution

geometry, the testing machine (hydraulic jack) capacity, and the most convenient way of testing. The single-sided welded joint specimen was made using a continuous column of the total length of 1521 mm, while the beam (total length 1055 mm) was welded to the the column flange, Fig. 1.

The right side of Fig. 1 shows the manner in which the connection surface was prepared and the weld between the column flange and the beam executed. To avoid the brittle specimen failure through the joint weld, the weld was significantly oversized. In joint resistance design, the throat of the weld was taken to be 5 mm thick.

All specimen members (beams and columns) were made of the same steel grade S 235 JR +N. It is important to note that the places of purchase for these members were different, and they were ordered from three different manufacturers (A, B and C).

Combining the supplied members resulted in six nominally identical, but really different joint specimens. This opened the path to research on the influence of combinations of different geometrical and mechanical properties of the members on the behaviour, and the reliability of the joint analyzed. The mentioned combinations are clearly presented in Table 1.

Table 1 Welded joint specimen notations, depending on members combinations

Welded joint specimen ID	Column			Notations	
	A	B	C		
Beam	A	01_bAcA	02_bAcB	03_bAcC	b – beam; c – column; A , B and C – locations where the members were manufactured
	B	04_bBcA	05_bBcB	06_bBcC	

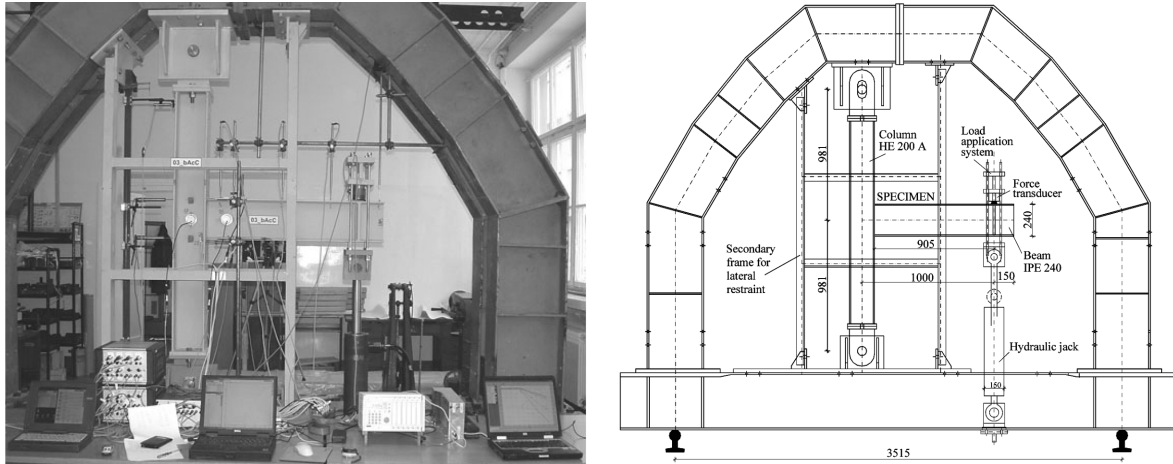


Fig. 2 Test arrangement

2.2.2 Test arrangement

The arrangement of specimens and testing equipment were shown in Fig. 2. The welded joint specimens were set so that the upper beam flange was in tension, and the lower in compression. The lower support is hinged, while the upper support is also hinged, but moveable in the vertical direction.

In order to prevent specimen failure due to lateral torsional buckling of members, the frames for lateral restraint were set so that the column is laterally restrained at the thirds of its length and the beam at half its length, somewhat closer to the point of loading.

2.2.3 Testing procedure

The load was applied by hydraulic jack with the capacity of 250 kN (tension) and maximum piston stroke of 400 mm in the point 1000 mm from the column axis, and 905 mm from the connection. Concentrated loading was enabled with a steel half-sphere welded on the upper beam flange, and 150 mm from the free end of the beam. The force transducer which ensures load measurement was placed on a steel half-sphere 25 mm in diameter so that it was using a calotte adapter – in that way ensuring a constant vertical force loading regardless of beam deflection. A detailed display of the loading application system was given in Fig. 3.

The specimens were subjected to monotonic force, which was applied to the beam by means of hydraulic jack. The tests were carried out under load control with a constant speed of $0.06 \text{ kN/s} = 3.6 \text{ kN/min}$ up to the collapse of the specimens. The test began with the first step of loading up to $2/3 M_{j,Rd}$ ($\sim 29 \text{ kNm}$), which represents the theoretical elastic limit (elastic joint moment resistance). The full plastic joint moment resistance, $M_{j,Rd}$, was determined according to Eurocode 3, Part 1.8 (CEN 2005).

After a 5 min pause complete unloading (second loading step) followed. The specimens were then reloaded up to the collapse, so that cca 3 min pauses were made at the following load levels, which correspond to the $2/3 M_{j,Rd}$ and the $M_{j,Rd}$. In the knee range (KR) and after this range the pauses were made every 0.5 min.

The knee-range of $M_j-\phi$ curve corresponds to the transition from the stiff to the soft part, Fig. 4. The test hold on lasted 3 min and was performed to record the quasi-static forces.

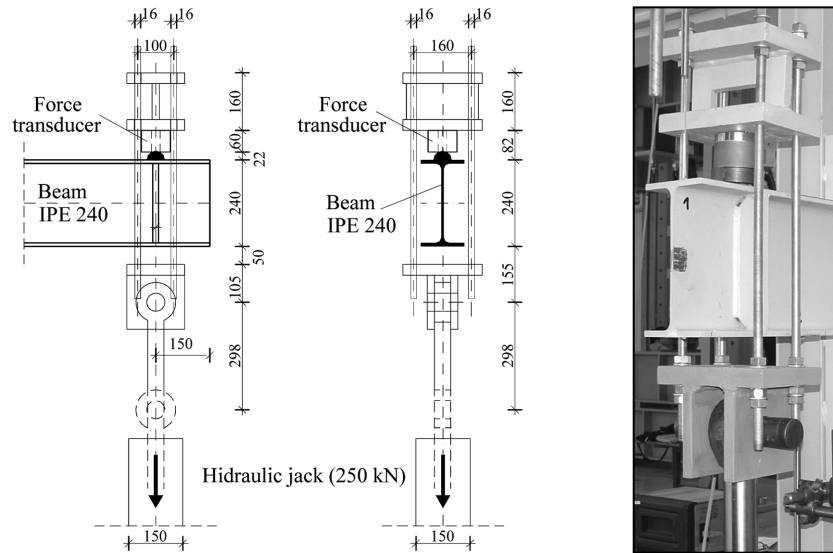
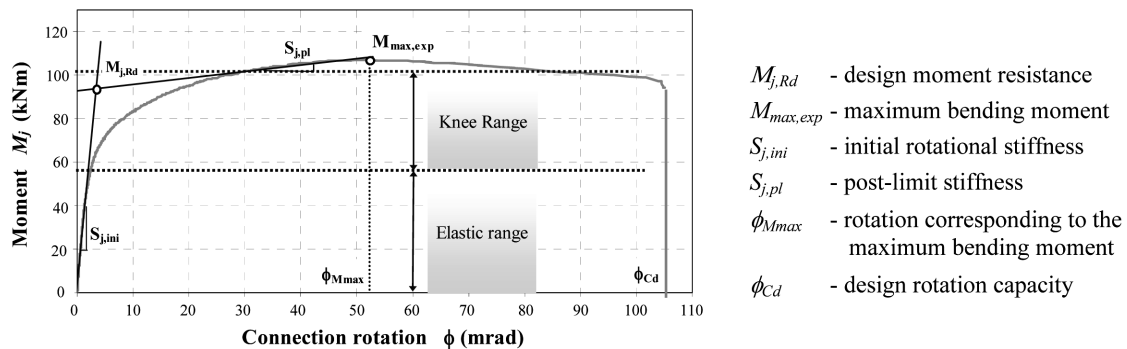


Fig. 3 The load application system

Fig. 4 Moment-rotation (M_j - ϕ) characteristics (illustration with specimen 03_bAcC)

2.2.4 Arrangement of the instrumentation

In order to record real joint behaviour it is necessary to measure the values of loading, beam rotation, column rotation, joint compression zone deformation, joint tension zone deformation, column web panel shear deformation and the corresponding rotation.

All welded beam-to-column joint specimens were tested using the same number, location and type of measurement devices. The arrangement of all measurement devices is shown in Fig. 5 and Fig. 6.

The displacements were measured by means of Linear Variable Displacement Transducers (LVDTs, CH1-CH16), placed as indicated on Fig. 5. Column and beam axis rotation was also recorded through inclinometers (CH17 and CH18). Strain gauges were set into the center of joint (CH19-CH21), the column web compression zone (CH22-CH24) and the tensional beam flange (CH25 and CH26) to record deformation states and to provide insight into the strain distribution of those zones. The locations of strain gauges were determined based on preliminary analyses in nonlinear finite element software - COSMOSM (2005).

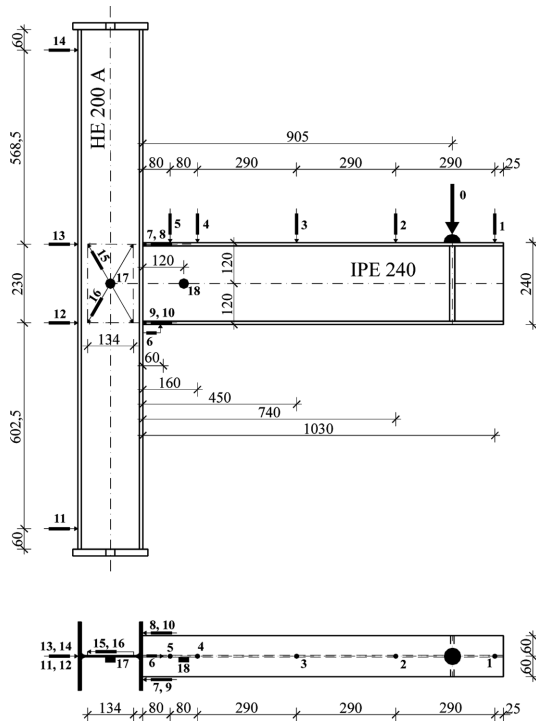


Fig. 5 Location of the force transducer (CH0), displacement transducers (CH1-CH16), and inclinometers (CH17-CH18)

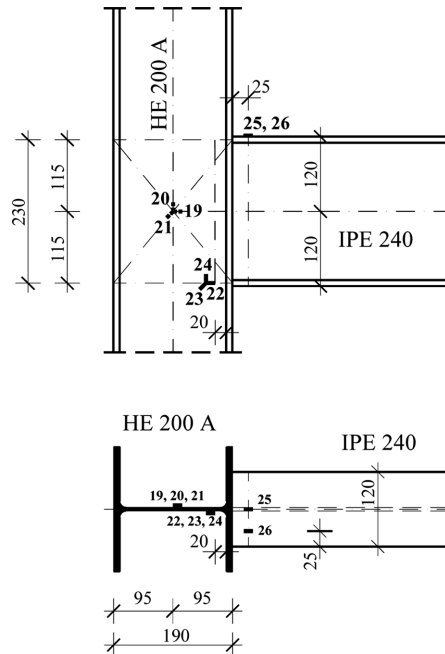


Fig. 6 Location of the strain gauges (CH19-CH26)

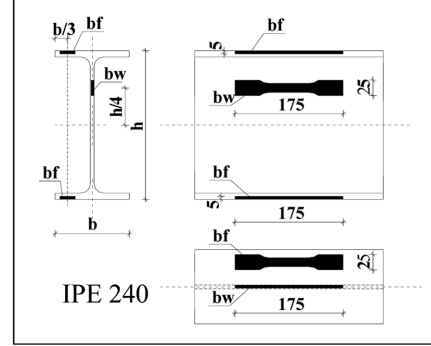
2.3 The mechanical properties of structural steel

The mechanical properties of the steel were tested according to European Standards EN 10002-Part 1 (CEN 1990) using 18 test pieces of the same shape and dimensions, regardless of the place where they were taken out of the member, section type and location where they were purchased. Three test pieces were taken from the IPE 240 beam section, Fig. 7(a), two from the flanges (f) and one from the web (w). Four test pieces were taken from the HE 200 A column section, Fig. 7(b), two from the flanges (f), one from the web parallel to the rolling direction (w_1), and one from the web perpendicular to the rolling direction (w_2). Table 2 gives the mechanical properties for the steel.

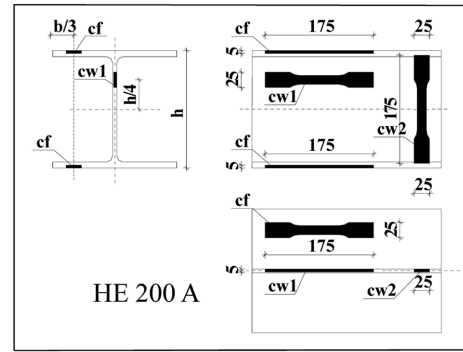
Test pieces from webs generally have higher yield strength, than the test pieces from the flanges. The differences in strength are somewhat less obvious, especially in IPE 240 beams. Test results for test pieces from IPE 240 beams flanges and webs for both A and B manufacturing locations fit each other rather well. It can be concluded that mechanical properties in the beam cross-section are much more consistent than in the HE 200 A section, out of which the joint specimens columns were made. The differences between the obtained yield strengths and corresponding strengths are large, and the ratio of the mean values of f_u and f_y equals about 1.42 (469/331) and expresses significant ductility of steel. Based on this, a significant rotational capacity of the joint is also to be expected. However a good material ductility does not necessarily imply that the whole structure is ductile, because the structural ductility depends on the structural discontinuities (welds, bolt holes, etc.).

Table 2 The values of main mechanical properties

Test piece		f_y [MPa]	f_u [MPa]	ε [%]	
Beam IPE 240	A	01_bAf	299	428	26.6
		02_bAf	305	436	27.6
		03_bAw	309	427	33.8
	B	04_bBf	336	482	27.4
		05_bBf	336	481	29.9
		06_bBw	361	486	32.3
Column HE 200 A	A	07_cAf	341	483	24.2
		08_cAf	342	483	26.9
		09_cAw1	405	516	23.7
		10_cAw2	374	490	28.9
	B	11_cBf	321	478	31.5
		12_cBf	333	481	32.2
		13_cBw1	336	507	15.9
		14_cBw2	352	502	24.7
	C	15_cCf	288	432	33.9
		16_cCf	284	431	29.7
	17_cCw1	341	464	28.8	
	18_cCw2	302	443	34.1	
Mean value μ		331	469	28.4	
Standard deviation σ		30.91	29.15	4.54	



(a) location of samples to be taken for beam



(b) location of samples to be taken for column

Fig. 7 Position of test pieces

3. Test results evaluation

3.1 Joint rotation

3.1.1 Total joint rotation

The total joint rotation including the elastic beam rotation, $\Phi_{tot} = Rot b$, can be calculated from the vertical displacement of beam at five different points LVDT 1-5 (Fig. 5), and is given by

$$\Phi_{tot} = Rot b = \arctan \frac{\delta_{LVDT,1}}{1030} = \arctan \frac{\delta_{LVDT,2}}{740} = \arctan \frac{\delta_{LVDT,3}}{450} = \arctan \frac{\delta_{LVDT,4}}{160} = \arctan \frac{\delta_{LVDT,5}}{80} \quad (1)$$

where $\delta_{LVDT,i}$ is the vertical displacement of the i^{th} LVDT, see Fig. 8. The expression above disregards the effect of shear deformation in the beam.

Moment - rotation from the Fig. 9 shows the total rotation in the example of the 03_bAcC joint. Rotation obtained from LVDT 5 ($Rot b_5$) significantly deviates from rotations obtained from other LVDT-s. This was to be expected, since the LVDT 5 was placed near the connection, where beam theory is no longer valid, and the stress distribution is not smooth. As other LVDT results are equal with an accuracy that is satisfactory, further experimental results evaluation is continued with Rot

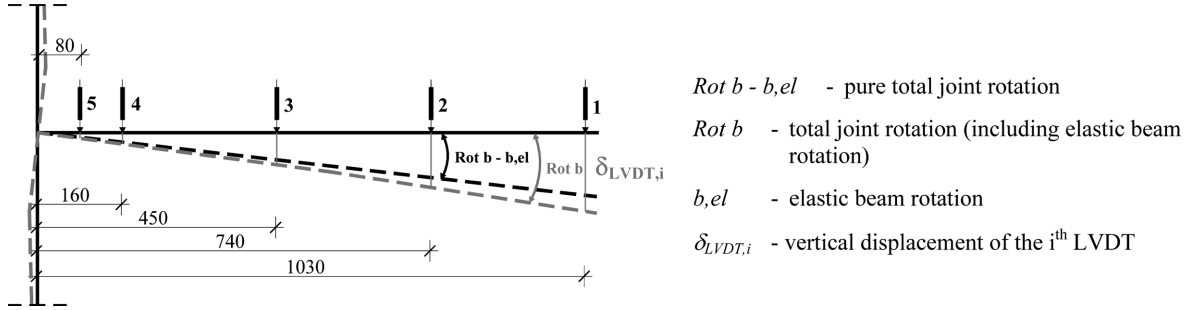


Fig. 8 Determining the total joint rotation

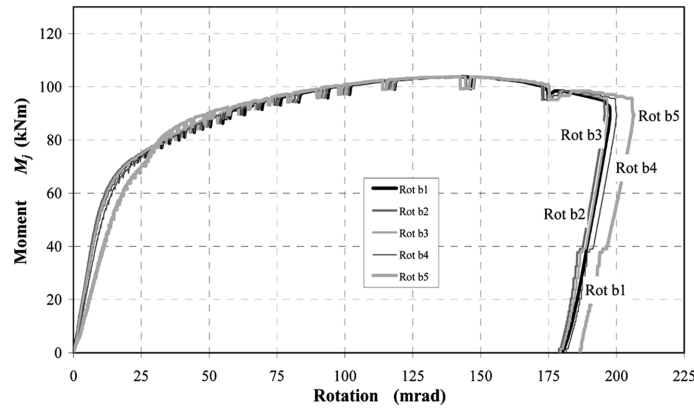
03_bAcC_full Moment - total joint rotation, $\Phi_{tot} = Rot\ b$ 

Fig. 9 Total joint rotation including elastic beam rotation

$b1$, or the rotation calculated from LVDT 1 measuring vertical displacement at the point near the end of the beam.

When the elastic beam rotation is subtracted from the total joint rotation, as shown in Fig. 8, (elastic column rotation is disregarded), the pure total rotation, Φ , is obtained

$$\Phi = Rot\ b1 - b,el = \arctan \frac{\delta_{LVDT1}}{1030} - \theta_{b,el} \quad (2)$$

In expression (2) the elastic beam rotation at the load application point is $\theta_{b,el} = b,el = \frac{FL_F^2}{2E_b I_b}$, where

F - applied force,

L_F - distance between the load application point and connection,

E_b - Young modulus of a beam,

I_b - second moment of area of beam.

The influence of beam elastic deformation on total joint rotation, Fig. 10, is dependant on the force F applied at the end of the beam, L_F .

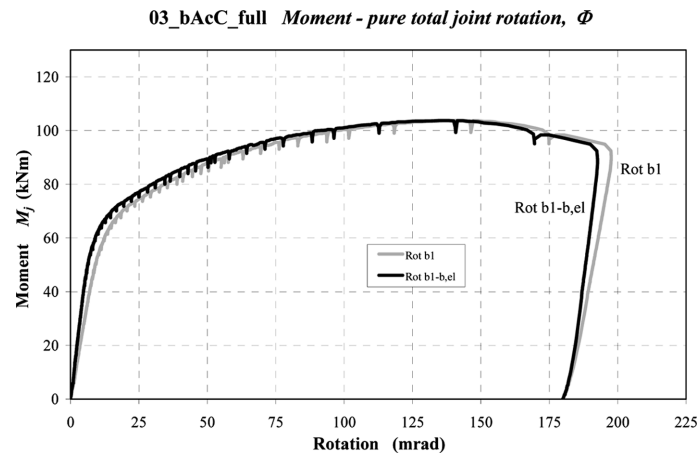


Fig. 10 Influence of beam elastic rotation on total joint rotation

3.1.2 Shear deformation of the column web panel zone

The shear deformation of the column web panel zone was calculated using the displacements measured by LVDTs 12 and 13. At first the displacement, $\Delta H1$, was obtained, Fig. 11, representing the difference between the horizontal displacement at the level of the tensional flange centreline, $w13$, and the horizontal displacement at the level of the compressional flange centreline, $w12$.

When the difference between displacements, $\Delta H1$, is divided by the distance between LVDT 12 and 13, the shear deformation of the column web panel zone (including elastic rotations of the column in that area), γ , is obtained, and marked as $Rot H1$ in Fig. 12.

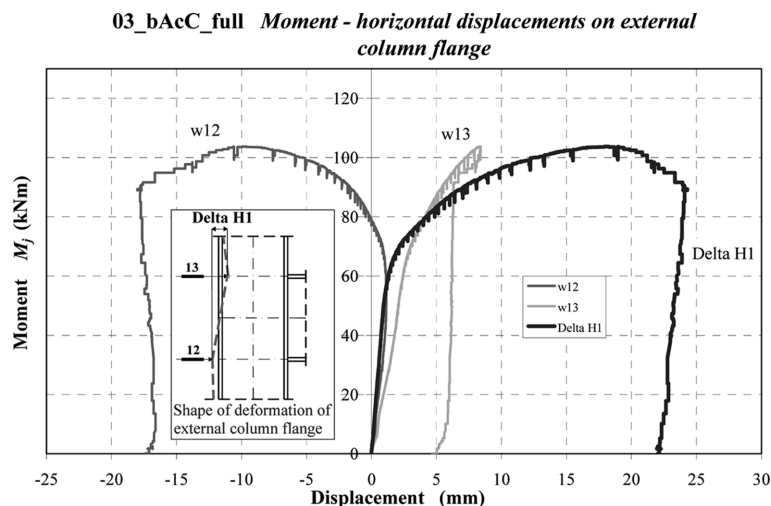


Fig. 11 The difference between horizontal displacements at LVDT12 and LVDT13 on column external flange, $\Delta H1$

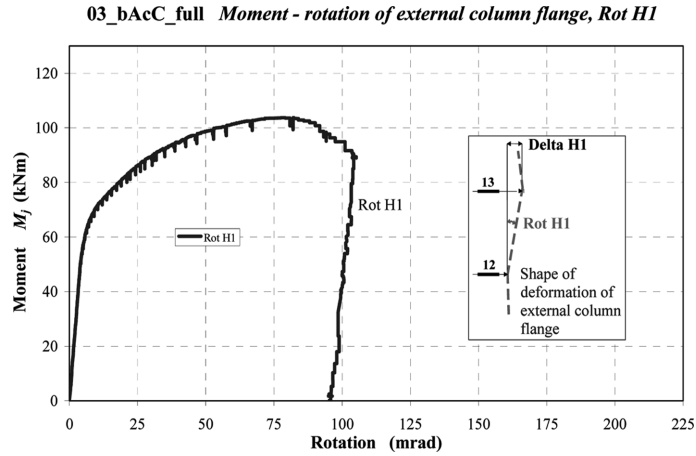


Fig. 12 Column web panel shear deformation (rotation), *Rot H1*

3.1.3 Connection rotation

The rotation of joint, Φ , is the sum of the shear deformation of the column web panel zone, γ , and the connection rotational deformation, ϕ , (Jaspart 1997). The connection rotation, ϕ , is defined as the change in the angle between beam and column centrelines, θ_b and θ_c

$$\phi = \theta_b - \theta_c \tag{3}$$

In the tests conducted both the column and the beam have been deformed, so the connection rotation can be obtained by subtracting the rotation caused by the shear on the column web panel zone, from the pure joint rotation, Fig. 13. So connection rotation, ϕ , (in the Fig. 14 denoted as Rot) can be expressed as

$$\phi = \Phi - \gamma, \text{ or} \tag{4}$$

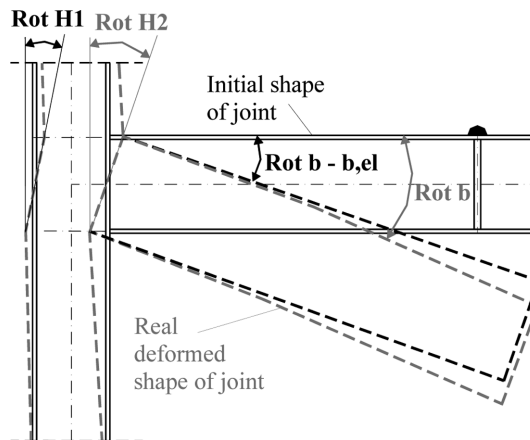


Fig. 13 Different rotations used on determining the connection rotation

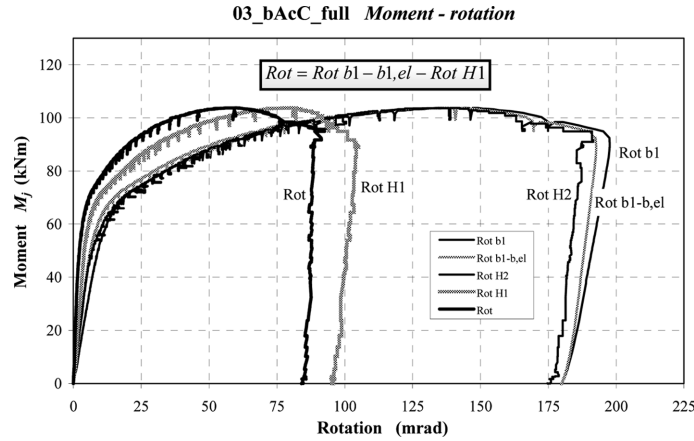


Fig. 14 Moment-rotation curves for different rotations

$$Rot = Rot\ b1, \ el - Rot\ H1 = \arctan \frac{\delta_{LVDT,1}}{1030} - \theta_{b,el} - \frac{\delta_{LVDT,13} - \delta_{LVDT,12}}{z} \quad (5)$$

In the expression above:

$\delta_{LVDT,13}$, $\delta_{LVDT,12}$ - displacements at LVDT 13, and LVDT 12; marked as $w13$ and $w12$ onward for the sake of simplicity,

z - distance between centrelines of beam flanges (the distance between LVDTs 12 and 13).

Other marks are already familiar, while Fig. 13 clearly shows different rotations in Eq. (5).

Fig. 14 shows *Rot H2* which represents the rotation at the place where the beam connects with the column flange, Fig. 13. As can be seen, that rotation is somewhat lower than the total joint rotation since it does not include the influence of the component - the beam flange and web in compression. *Rot H2* presents important data exactly because of the fact mentioned - this allows a quantitative differentiation between column and beam influences on the behaviour of the whole joint.

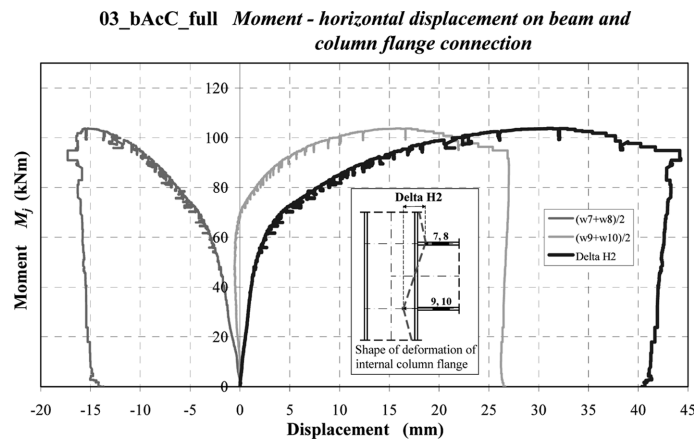


Fig. 15 The difference between averaged horizontal displacements at LVDT7-8 and LVDT9-10 on beam and column flange connection, *Delta H2*

Rotation on the beam and column flange connection, *Rot H2*, can be obtained as follows: *Delta H2*, see Fig. 15, is obtained as the difference between averaged horizontal displacements on the connection, at the level of the beam flanges centrelines. Then the *Delta H2* is divided with the distance between flanges centrelines. The result equals *Rot H2*, the rotation on the connection shown in Fig. 14.

4. Discussion of test results

4.1 The models for experimental moment resistance determination

In evaluating test results which would provide experimental plastic moment resistance, $M_{p,exp}$, four models have been applied (Skejic 2005), as shown in Table 3, or Fig. 16. A lots of models exist which can characterize the experimental $M_j-\phi$ curves (Szelendak 2002). In this paper two simple models are applied, the EC3-A and EC3-B, Table 2, which cannot be found in the relevant literature, and characterize the real joint type behaviour very well. The ‘Knee range’ model has been applied in evaluating the test results for bolted beam-to-column joints with a extended end plate (Girao Coelho *et al.* 2004). Based on that model the plastic joint moment resistance can be determined as the intersection between the line with the slope coefficient, $S_{j,ini,exp}$, and the linearized $M_j-\phi$ curve in the area behind knee range up to maximum bending moment, $M_{max,exp}$. The traditional EC3 model was used in the SERICON database evaluation, and is based on the simple idea of intersecting the secant rotational stiffness, $S_{j,ini,exp}/3$, with the $M_j-\phi$ curve (Cruz *at al.* 1998).

In Table 3, $S_{j,ini,exp}$ stands for the experimental initial rotational stiffness, and was obtained as the slope coefficient of the linearized part of the $M_j-\phi$ curve, from the beginning of the curve to the point where the knee range begins, see Fig. 16. When determining the beginning and end of the

Table 3 Models for determining of $M_{p,exp}$ (Skejic 2005)

The $M_{p,exp}$ determination model	Model description
EC3 – A	$M_{p,exp,EC3-A}$ represents intersection between the line y (with the slope coefficient $S_{j,ini,exp}$) and the linearized part of $M_j-\phi$ curve, denoted as y_{EC3-A} , see Fig. 16(a). The linearized part of $M_j-\phi$ curve in this model corresponds to the part behind the intersection of line y_{EC3} (with the slope coefficient $S_{j,ini,exp}/3$) and $M_j-\phi$ curve till the end of knee range.
EC3 - B	$M_{p,exp,EC3-B}$ represents intersection between the line y (with the slope coefficient $S_{j,ini,exp}$) and the linearized part of $M_j-\phi$ curve, denoted as y_{EC3-B} , see Fig. 16(b). The linearized part of $M_j-\phi$ curve in this model corresponds to the part behind the intersection of line y_{EC3} (with the slope coefficient $S_{j,ini,exp}/3$) and $M_j-\phi$ curve till the $M_{max,exp}$.
Knee range	$M_{p,exp,KR}$ represents intersection between the line y (with the slope coefficient $S_{j,ini,exp}$) and the linearized part of $M_j-\phi$ curve, denoted as y_{KR} , see Fig. 16(c). The linearized part of $M_j-\phi$ curve in this model corresponds to the part behind knee range till $M_{max,exp}$.
EC3	$M_{p,exp,EC3}$ represents intersection between the line y_{EC3} (with the slope coefficient $S_{j,ini,exp}/3$) and the $M_j-\phi$ curve, see Fig. 16(d).

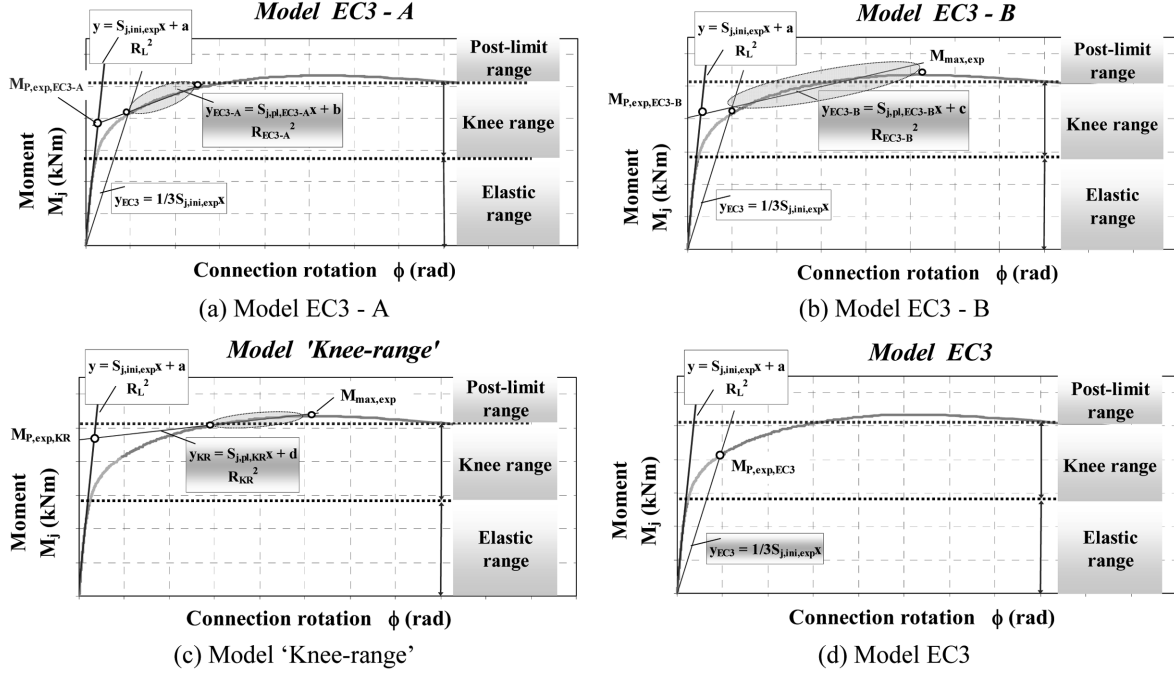


Fig. 16 Models for experimental moment resistance determination, in the example of the specimen 03_bAcC

knee range, the guiding idea was that these characteristic points would be determined from the experimental M_j - ϕ curve as the points which correspond to the transition from the stiff, and into the soft part, respectively. The criteria used was that the R -squared value, R_L^2 , would not drop below 0.95 for the linearization of the initial, elastic part, and that R_{KR}^2 would not drop below 0.90. The knee range is where the joint stiffness constantly decreases. Leaving the knee range the joint enters a post-limit range, where it holds constant post-limit stiffness, $S_{j,pl}$ almost up to the maximum experimental bending moment, $M_{max,exp}$. The post-limit stiffness is defined depending on the model used in the experimental moment resistance determination. Fig. 16(c) shows it as the slope coefficient of the linearized part of M_j - ϕ curve in the post-limit range, $S_{j,pl,KR}$.

It is important to mention here that various methodologies are used in the relevant literature for analyzing experimental data on semi rigid joint behaviour, and each of them has its advantages, setbacks and limits within which they possess physical justification. The conclusion can then be drawn that the choice of an appropriate model for determining the experimental moment resistance is primarily defined by joint type and configuration, as well as the type and function of the structural frame system to which the joint belongs.

4.2 Test results

All tested specimens failed through the component column web in transverse compression. Typical failure mode (specimen 03_bAcC) is shown in Fig. 17.

Different M_j - ϕ curves were obtained for all six nominally identical specimens of the welded semi rigid beam-to-column joint, Fig. 18. The differences were primarily caused by the fact that the joint specimens were composed of members, both beams and columns, provided by different European

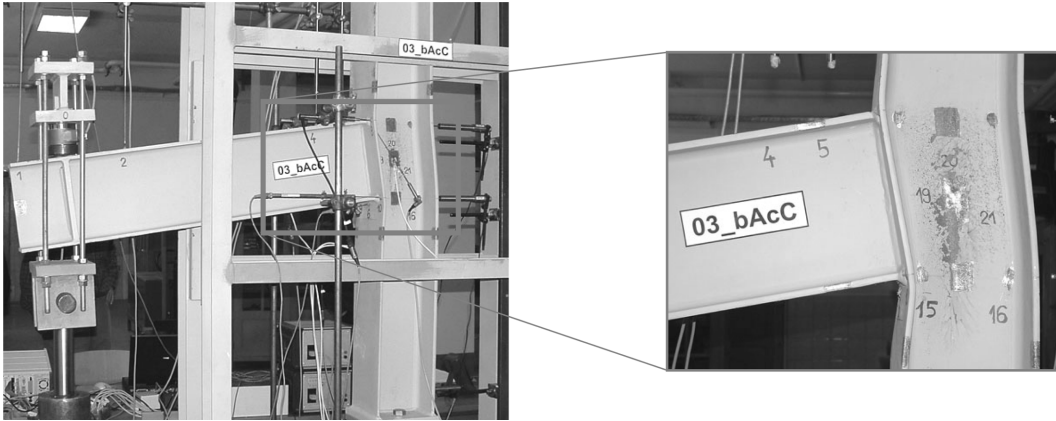
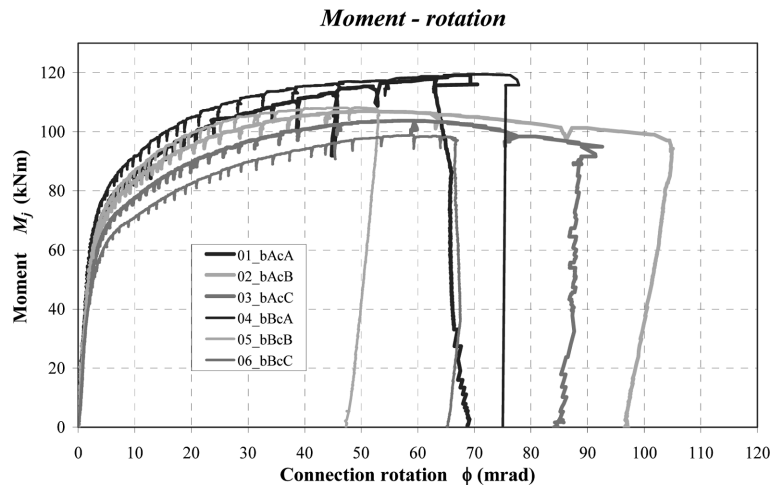


Fig. 17 Specimen 03_bAcC after the failure

Fig. 18 Moment-rotation (M_j - ϕ) curves

steel I section manufacturers, so the nominally identical specimens differed in both mechanical and geometrical properties.

The results can, finally, be grouped into three groups, depending on the location of column manufacture. The first group consists of specimens 01_bAcA and 04_bBcA, the second of 02_bAcB and 05_bBcB, and the third of 03_bAcC, as well as 06_bBcC. This is justified by the fact that the fifth component - beam flange and web in compression is dominant. Based on that, the beam as a member has no major influence on the behaviour of the considered joint type.

The evaluated test results which characterize the M_j - ϕ curves obtained are shown in Tables 4 to 6, depending on the model for experimental moment resistance determination. Those tables also show ratios which describe the real behaviour of tested welded beam-to-column joints in even more detail, with regard to the theoretical values obtained in the semi-probabilistic analysis conducted according to EC3, Part 1.8 (CEN 2005).

Table 4 Test results for moment resistance

Specimen	Model	$M_{j,R}$ (kNm)	M_P (kNm)	$\frac{M_P}{M_{j,R}}$	$M_{P,exp}$ (kNm)	$\frac{M_{P,exp}}{M_{j,R}}$	$\frac{M_{P,exp}}{M_P}$	$M_{max,exp}$ (kNm)	$\frac{M_{max,exp}}{M_{P,exp}}$
01_bAcA	EC3 - A	48.90	75.79	1.55	81.04	1.66	1.07	119.23	1.47
	EC3 - B				88.26	1.80	1.16		1.35
	Knee range				97.32	1.99	1.28		1.23
	EC3				87.83	1.80	1.16		1.36
02_bAcB	EC3 - A	48.90	72.76	1.49	76.64	1.57	1.05	106.99	1.40
	EC3 - B				82.60	1.69	1.14		1.30
	Knee range				93.92	1.92	1.29		1.14
	EC3				82.74	1.69	1.14		1.29
03_bAcC	EC3 - A	48.90	65.70	1.34	69.27	1.42	1.05	103.75	1.50
	EC3 - B				75.77	1.55	1.15		1.37
	Knee range				86.27	1.76	1.31		1.20
	EC3				76.05	1.56	1.16		1.36
04_bBcA	EC3 - A	48.90	78.89	1.61	83.11	1.70	1.05	119.42	1.44
	EC3 - B				93.62	1.91	1.19		1.28
	Knee range				105.65	2.16	1.34		1.13
	EC3				91.81	1.88	1.16		1.30
05_bBcB	EC3 - A	48.90	71.82	1.47	80.28	1.64	1.12	108.22	1.35
	EC3 - B				87.06	1.78	1.21		1.24
	Knee range				99.32	2.03	1.38		1.09
	EC3				87.36	1.79	1.22		1.24
06_bBcC	EC3 - A	48.90	64.04	1.31	64.94	1.33	1.01	98.85	1.52
	EC3 - B				71.20	1.46	1.11		1.39
	Knee range				80.22	1.64	1.25		1.23
	EC3				72.33	1.48	1.13		1.37
Mean value	EC3 - A	48.90	71.50	1.46	75.88	1.55	1.06	109.41	1.45
	EC3 - B				83.09	1.70	1.16		1.32
	Knee range				93.78	1.92	1.31		1.17
	EC3				83.02	1.70	1.16		1.32

Table 4 gives the results related to joint moment resistance. The characteristic plastic joint moment resistance, $M_{j,R}$, was calculated according to EN 1993, Part 1.8 ($M_{j,R} = M_{j,Rd} \cdot \gamma_M$, where $M_{j,Rd}$ is the design moment resistance and γ_M is the partial factor and was taken to equal 1.0). Plastic moment resistance, M_P , was calculated in the same way as $M_{j,R}$ but using the measured mechanical and geometrical properties. The experimental plastic joint moment resistance, obtained according to adopted models, is marked $M_{P,exp}$, while the maximum moment recorded in the tests is marked $M_{max,exp}$.

The EC3 – A model gives the lowest moment resistance, $M_{P,exp}$, while the ‘Knee Range’ model gives the highest moment resistance. The EC3 – B and the EC3 model both give an almost identical mean value of $M_{P,exp}$, of around 83 kNm. This is 1.70 times higher than the $M_{j,R}$ and 1.16 times

Table 5 Test results for rotational stiffness

Specimen	Model	$S_{j,ini}$ (kNm/rad)	$S_{j,ini}^*$ (kNm/rad)	$S_{j,ini,exp}$ (kNm/rad)	$\frac{S_{j,ini,exp}}{S_{j,ini}}$	$\frac{S_{j,ini,exp}}{S_{j,ini}^*}$	$S_{j,pl}$ (kNm/rad)	$\frac{S_{j,pl}}{S_{j,ini,exp}}$
01_bAcA	EC3 - A	16309	17564	23810	1.46	1.36	1042.1	22.85
	EC3 - B						592.21	40.21
	Knee range						370.16	64.32
	EC3						0.00	
02_bAcB	EC3 - A	16309	17516	26257	1.61	1.50	1064.9	24.66
	EC3 - B						632.35	41.52
	Knee range						298.24	88.04
	EC3						0.00	
03_bAcC	EC3 - A	16309	16903	25877	1.59	1.53	1194.2	21.67
	EC3 - B						673.80	38.40
	Knee range						373.43	69.30
	EC3						0.00	
04_bBcA	EC3 - A	16309	17704	28029	1.72	1.58	1286.0	21.80
	EC3 - B						509.39	55.02
	Knee range						219.71	127.57
	EC3						0.00	
05_bBcB	EC3 - A	16309	17368	26032	1.60	1.50	1105.2	23.55
	EC3 - B						599.32	43.44
	Knee range						218.51	119.13
	EC3						0.00	
06_bBcC	EC3 - A	16309	16618	21409	1.31	1.29	1014.7	21.10
	EC3 - B						598.01	35.80
	Knee range						369.50	57.94
	EC3						0.00	
Mean value	EC3 - A	16309	17279	25236	1.55	1.46	1117.85	22.60
	EC3 - B						600.85	42.40
	Knee range						308.26	87.72
	EC3						0.00	

higher than the M_p . The mean maximum moment determined in the tests, $M_{max,exp}$, is on average 1.32 times higher than the experimentally determined plastic moment resistance, $M_{p,exp}$, based on the EC3 – B model.

The test results which concern rotational stiffness are given in Table 5. Initial rotational stiffness, $S_{j,ini}$, was obtained according to EN 1993, Part 1.8. When the initial rotational stiffness is calculated using the measured mechanical and geometrical properties, $S_{j,ini}^*$ is obtained. The experimental $M_j-\phi$ curves provide the initial rotational stiffness $S_{j,ini,exp}$, and post-limit stiffness, $S_{j,pl}$. The post-limit stiffness, $S_{j,pl}$, is dependant on the moment resistance determination model.

The mean value of the ratio of the experimentally determined initial stiffness, $S_{j,ini,exp}$, and the theoretical value with measured properties, $S_{j,ini}^*$, equals 1,46. Initial rotational stiffness for the

Table 6 Test results for rotation capacity

Specimen	Model	ϕ_{Cd} (mrad)	$\phi_{MP,exp}$ (mrad)	$\phi_{Mmax,exp}$ (mrad)	$\phi_{Cd,exp}$ (mrad)
01_bAcA	EC3 - A	10.00	3.24	67.25	69.28
	EC3 - B		3.54		
	Knee range		3.92		
	EC3		11.00		
02_bAcB	EC3 - A	10.00	2.77	52.93	105.03
	EC3 - B		3.00		
	Knee range		3.44		
	EC3		9.50		
03_bAcC	EC3 - A	10.00	2.67	58.79	92.57
	EC3 - B		2.93		
	Knee range		3.33		
	EC3		9.00		
04_bBcA	EC3 - A	10.00	2.79	72.22	77.87
	EC3 - B		3.17		
	Knee range		3.60		
	EC3		9.97		
05_bBcB	EC3 - A	10.00	2.92	49.73	53.00
	EC3 - B		3.18		
	Knee range		3.65		
	EC3		10.20		
06_bBcC	EC3 - A	10.00	2.94	58.84	66.67
	EC3 - B		3.24		
	Knee range		3.66		
	EC3		10.93		
Mean value	EC3 - A	10.00	2.89	59.96	77.40
	EC3 - B		3.18		
	Knee range		3.60		
	EC3		10.10		

tested joints, $S_{j,ini,exp}$, has been significantly underestimated in relation to theoretical values, $S_{j,ini}$. This can be concluded from the ratio of mean values $S_{j,ini,exp}$ and $S_{j,ini}$, which equals 1.55.

The joint post-limit rotational stiffness values must be analyzed based on the models applied for determining the moment resistance. Aside from the above, another important matter is that the slope of the post-limit part of the M_j - ϕ curve, $S_{j,pl}$, is determined by linearizing the curve part depending on the model for $M_{P,exp}$ determination (for more details, see Table 3 and Fig. 16). What can be said is that the rotational stiffness in the post-limit range, $S_{j,pl}$, is significantly lower than the recommended value $0,1S_{j,ini}$ (Aribert *et al.* 2004). The results of post-limit rotational stiffness need to be analyzed in more details, so that serviceability limit state criteria of the frame system are taken into account.

The results shown in Table 6 provide only indicative values, based on which conclusions may be drawn on the real rotation capacity of this type of joint. The ϕ_{Cd} in the Table 6 stands for rotation capacity according to CoP (Connection Program), with measured mechanical and geometrical properties (CoP, 2005). After evaluation the experimental M_j - ϕ curves, further experimental values for the rotation $\phi_{MP,exp}$, $\phi_{Mmax,exp}$, equaling respectively the level of $M_{P,exp}$ and the level of maximum moment, $M_{max,exp}$, have been obtained.

The values of rotation capacity obtained from tests are significantly higher than the minimum rotation capacity values proposed in EN 1993, Part 1.8 (CEN 2005), equaling 15 mrad. Based on the design rotation capacity values equaling 10 mrad (according to CoP 2005), can be said to be significantly underestimated, when using the present component method, Table 6.

Furthermore it is important to note that the tests were conducted using a constant loading speed for load control. Due to loading equipment limitations, the rotation capacity values are somewhat indicative, and vary from 53 mrad even to 105 mrad. The mean rotation capacity value equals 77.4 mrad.

5. Conclusions

The experimental testing of welded joint behaviour under static load was conducted on 6 nominally identical specimens. All of the specimens are actually different, being combined out of members manufactured around Europe. The specimens were designed for ductile failure through the column web under transverse compression. The following conclusions can be drawn from the tests:

1. Differences in the M_j - ϕ curves are primarily caused by the fact that the joints are made out of nominally identical members, which because of different manufacturers show extreme variability in mechanical and, to a lesser extent, geometrical properties.
2. With this joint configuration, the component - the beam flange and web in compression, and through it, the beam itself have very little influence on the behaviour of the joint type considered.
3. The most realistic model for determining the joint experimental plastic moment resistance was shown to be the EC3 – B. The simplified model, recommended by Eurocode 3, suits the EC3 – B model very well for the joint type tested.
4. Based on the mean value of the model factor ($M_{P,exp}/M_P$), which equals 1.16, it follows that the moment resistance according to the component method (EN 1993-1-8), was underestimated.
5. The mean value of the ratio between the experimentally determined and the theoretical initial stiffness with real properties ($S_{j,ini,exp}/S_{j,ini}^*$), equals 1.46, meaning the initial stiffness for this joint configuration has been significantly underestimated.
6. The loading of the specimens using load speed control is inadequate for ductile steel structural systems testing, so the rotation capacity results obtained represent only indicative values. None the less, they point to values up to 10 times higher than the design values calculated by CoP.
7. The mean value of the ratio $M_{max,exp}/M_{P,exp} = 1.32$, and high deformability, see Fig. 18, indicates high post-limit response of the tested joint. Therefore, for the more accurate prediction of the flexural behaviour of steel joints post-buckling models must be used.

Further research needs to be centered on the corrections and enhancements necessary to achieve a component method for other beam-to-column joint types and configurations acceptable to engineers.

Because a reliable joint classification is so important, and because of the consequences of a faulty classification on the calculation method choice, and in the end on the frame system reliability, the issue of the components method reliability carries still more weight, and requires a continuation of research using probabilistic reliability methods. It would also be interesting to perform a probabilistic comparison between different international standards for the calculation of semi rigid steel structure joints.

Acknowledgements

The financial support of the Ministry of Science, Education and Sports of Croatia through grant No. 0082214 is gratefully acknowledged.

References

- Aribert, J.-M., Braham, M. and Lachal, A. (2004), "Testing of "simple" joints and their characterisation for structural analysis", *J. Constr. Steel Res.*, **60**, 659-681.
- Beg, D., Zupančič, E. and Vayas, I. (2004), "On the rotation capacity of moment connections", *J. Constr. Steel Res.*, **60**, 601-620.
- CEN: European Committee for Standardization (1990), "EN 10002-1:1990E, Metallic materials – Tensile testing – Part 1: Method of test (at ambient temperature)", March, Brussels.
- CEN: European Committee for Standardization (2004), "EN 10204:2004, Metallic products", October, Brussels.
- CEN: European Committee for Standardization (2004), "EN 10025-2:2004, Hot rolled products of structural steels - Part 2", November, Brussels.
- CEN: European Committee for Standardization (2005), "EN 1993-1-8:2005, Eurocode 3: Design of steel structures, Part 1.8: Design of joints", May, Brussels.
- CoP (2005), Connection Program, Version 2005R02, RWTH Aachen, MSM Liège, ICCS Hoofddorp.
- COSMOSM (2005), GeoStar V2.95.
- Cruz, P.J.S., da Silva, L.S., Rodrigues, D.S. and Simões, R.A.D. (1998), "Database for the semi-rigid behaviour of beam-to-column connections in seismic regions", *J. Constr. Steel Res.*, **46**, 233-234.
- da Silva L.S., Santiago, A. and Vila Real, P. (2002), "Post-limit stiffness and ductility of end-plate beam-to-column steel joint", *Comp. Struct.*, **80**(5-6), 515-531.
- Girão Coelho, A.M., Bijlaard, F. S.K. and da Silva, L.S. (2004), "Experimental assessment of the ductility of extended end plate connections", *Eng. Struct.*, **26**, 1185-1206.
- Girão Coelho, A.M., da Silva, L.S. and Bijlaard, F.S.K. (2005), "Ductility analysis of end plate beam-to-column joints", *Proceedings of Eurosteel 2005*, Maastricht, 4.10, 123-130.
- Jaspart, J.P. (1997), "Contributions to recent advances in the field of steel joints, Column bases and further configurations for beam-to-column joints and beam splices", Aggregation thesis, University of Liège, Liège.
- Skejic, D. (2005), Master of Science Thesis, "Reliability of semi-rigid beam-to-column welded joints", Department of Structural Engineering, Faculty of Civil Engineering, University of Zagreb, Zagreb (in Croatian).
- Szlendak, J.K. (2002), "Design moment-rotation characteristics for steel semi-rigid beam-column joints", *Proceedings of Eurosteel 2002*, Coimbra, 1059-1066.